

Convective evolution, heating structures, and spin-up during rapid intensification under varying shear

Daniel S. Harnos and Stephen W. Nesbitt – Department of Atmospheric Sciences, University of Illinois at Urbana-Champaign



Motivations

Harnos and Nesbitt (2011) evaluated 20+ years of passive microwave satellite data and noted two structural modes at 85 GHz for TCs undergoing onset of rapid intensification (RI; $\Delta W_{24\text{ hr}} \geq 30 \text{ kt}$), dependent upon wind shear magnitude. Low shear exhibited a ring-like scattering signature associated with modest deep-convection whereas high shear exhibited an asymmetric and stronger scattering signature downshear. From observations, it is clear that ice-containing convection is present in a large majority of storms near RI onset.

“Convective bursts” or Vortical Hot Towers (VHTs) have been identified by several studies as playing a potential role in TC spinup, e.g.:

Nguyen et al. (2008); Montgomery and Smith (2011); Molinari and Vollaro (2010); McFarquhar et al. (2012)

We seek to evaluate how precipitation processes (i.e. convective bursts, deep convection, warm rain, and stratiform precipitation) evolve under varying shear, and these structures relate to RI onset.

Model Setup & Overview

Two TCs are simulated, Ike (2008) and Earl (2010), with low and high shear respectively, via version 3.3 of the WRF model.

- Domains: 27/9/3/1 km (1 km with preset moves)
- Vertical Levels: 55
- Boundaries/Initialization: ERA-Interim
- Microphysics: WRF Single Moment 6 Class
- Cumulus: Kain-Fritsch (27 km only)
- Planetary Boundary Layer: YSU
- Radiation (LW and SW): RRTMG

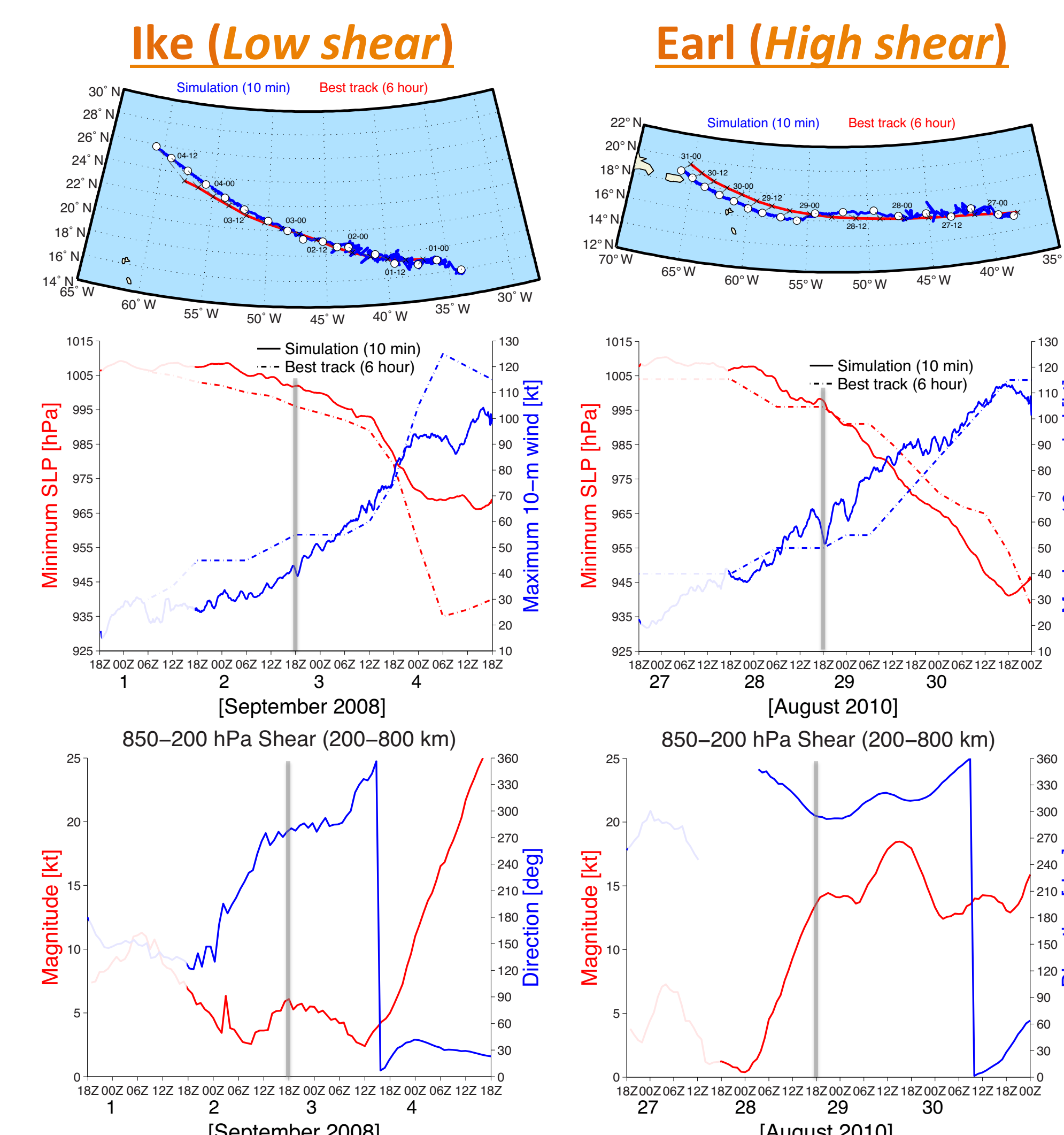


Fig. 1: Timeseries comparison of simulated track versus best track (top), simulated intensity versus best track intensity (middle), and simulated shear (bottom) for each system.

Results: Precipitation Coverage

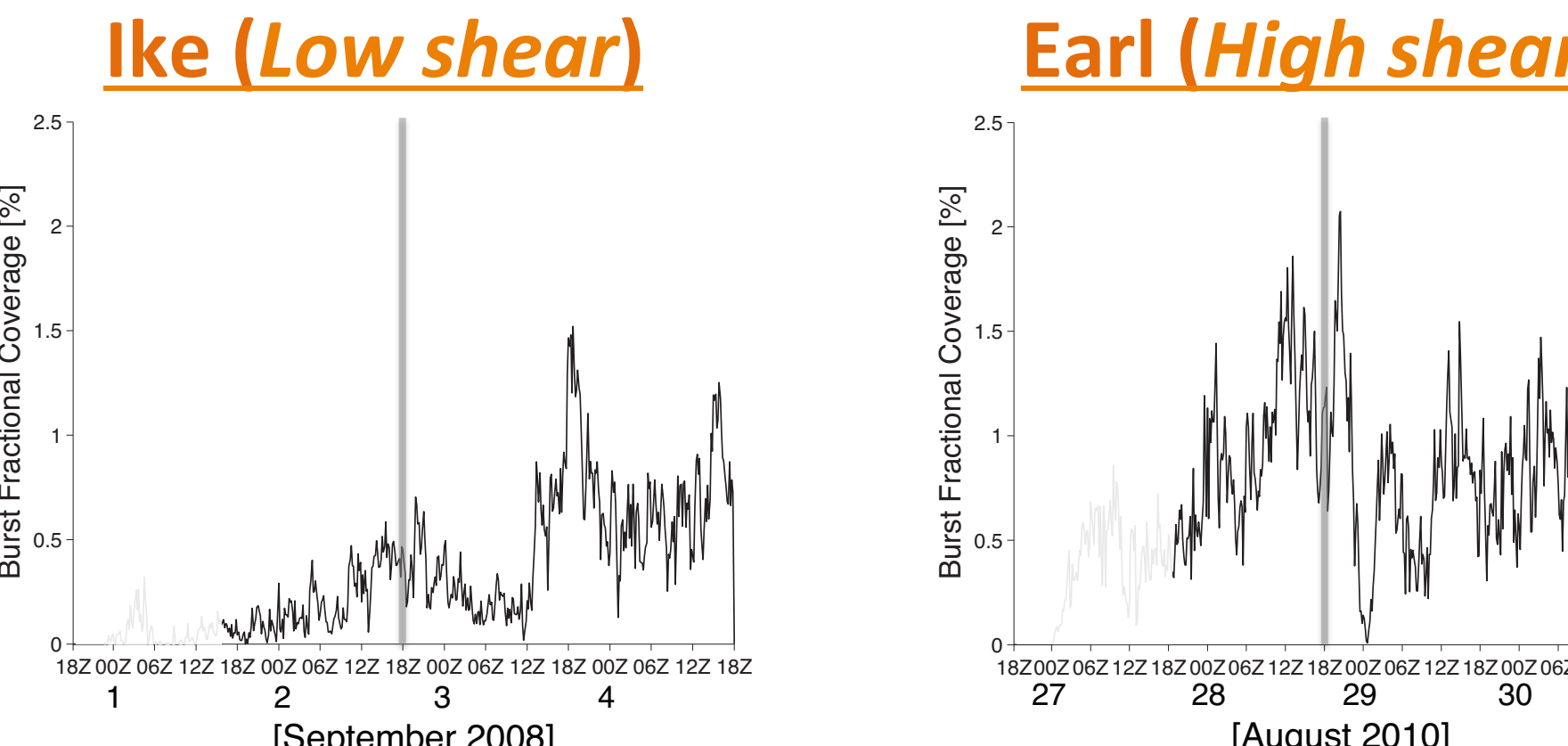


Fig. 2: Time series comparison of convective burst fractional coverage over the innermost 1°.

A burst is defined as in Rogers (2010) where $W_{700-300 \text{ hPa}} \geq 5 \text{ m s}^{-1}$.

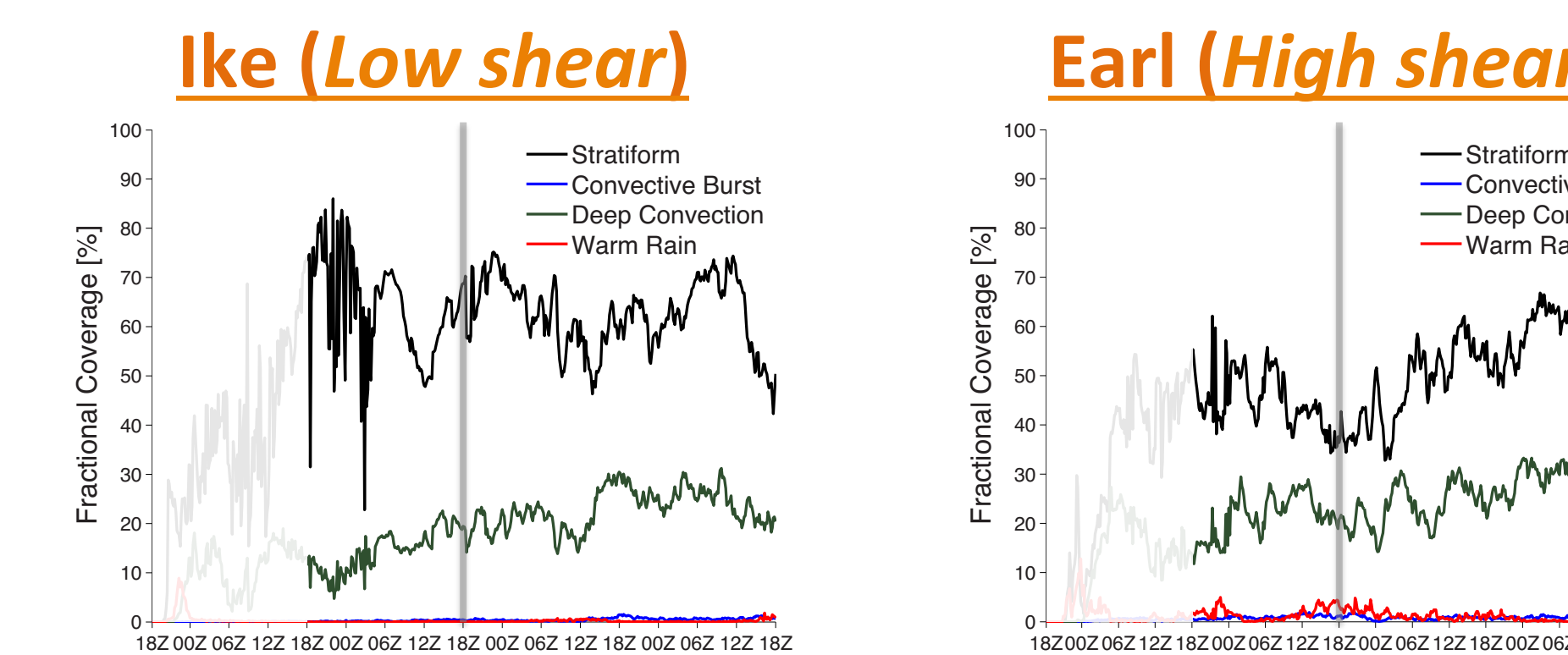


Fig. 3: Time series comparison of precipitation type fractional coverage over the innermost 1°.

Non-burst definitions are from a modified version of Steiner et al. (1995).

Results: Vortex Intensity

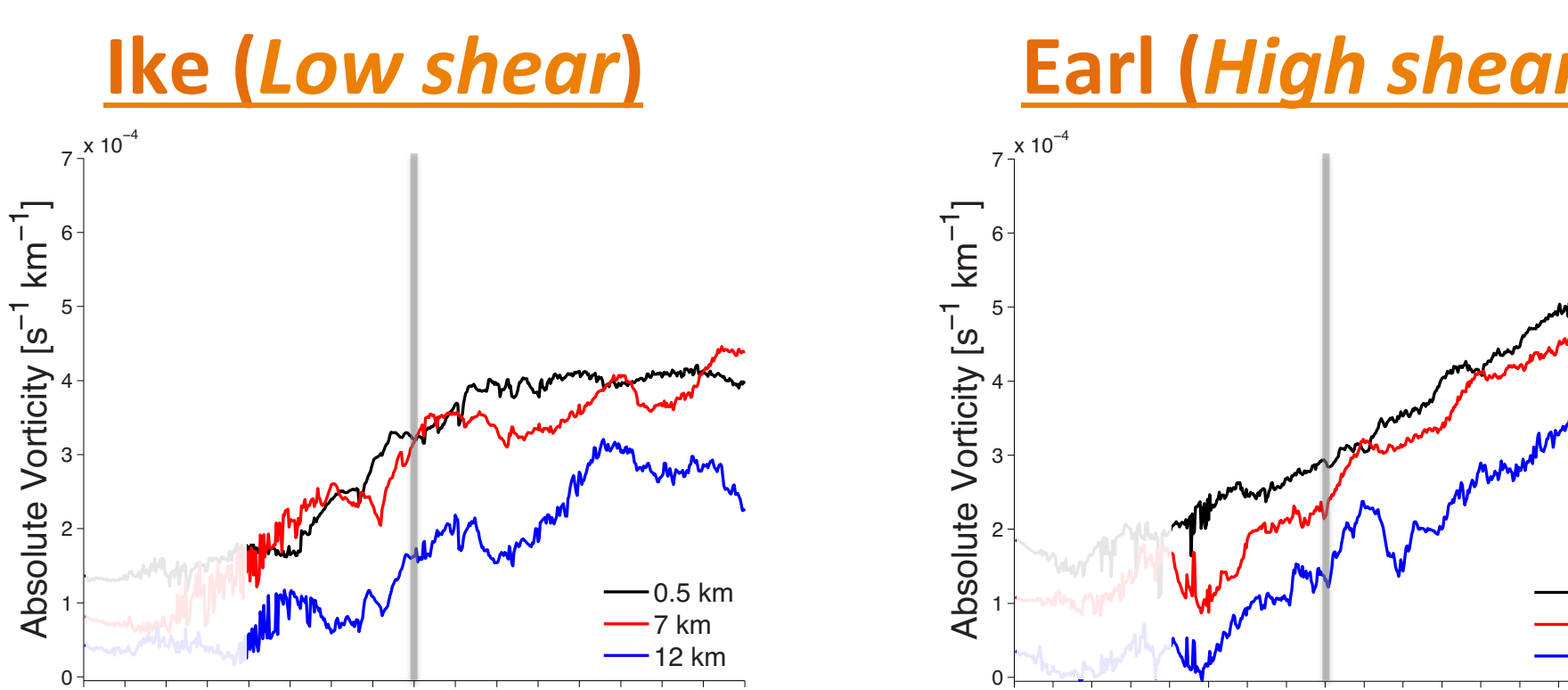


Fig. 7: Time series comparison of absolute vorticity over the innermost 1° at low- (0.5 km), mid- (7), and upper-levels (12 km).

Results: Spin-Up Contribution

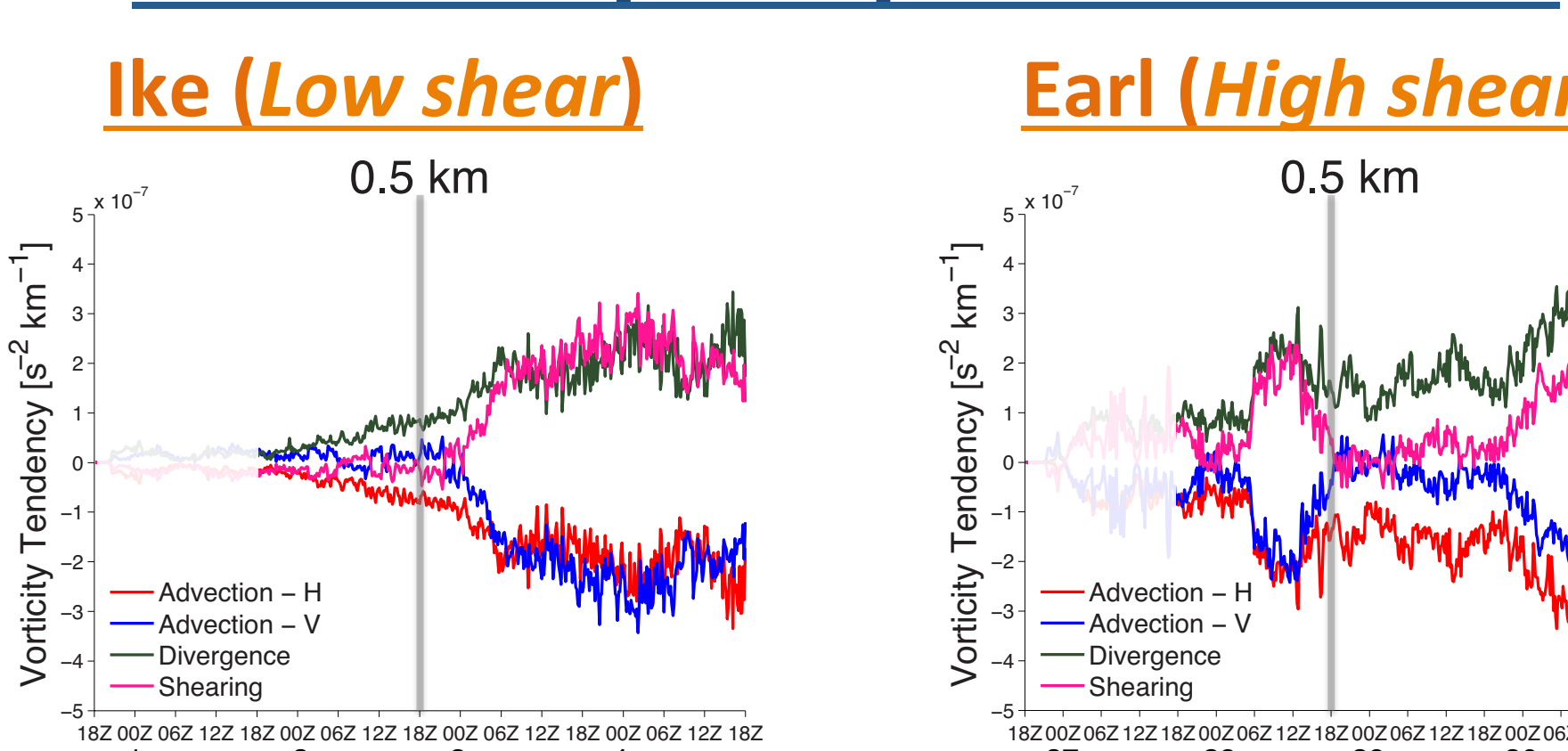


Fig. 8: Time series comparison by term of vorticity tendency contribution via the scaled vorticity equation in height coordinates.

Results: Convective Signatures

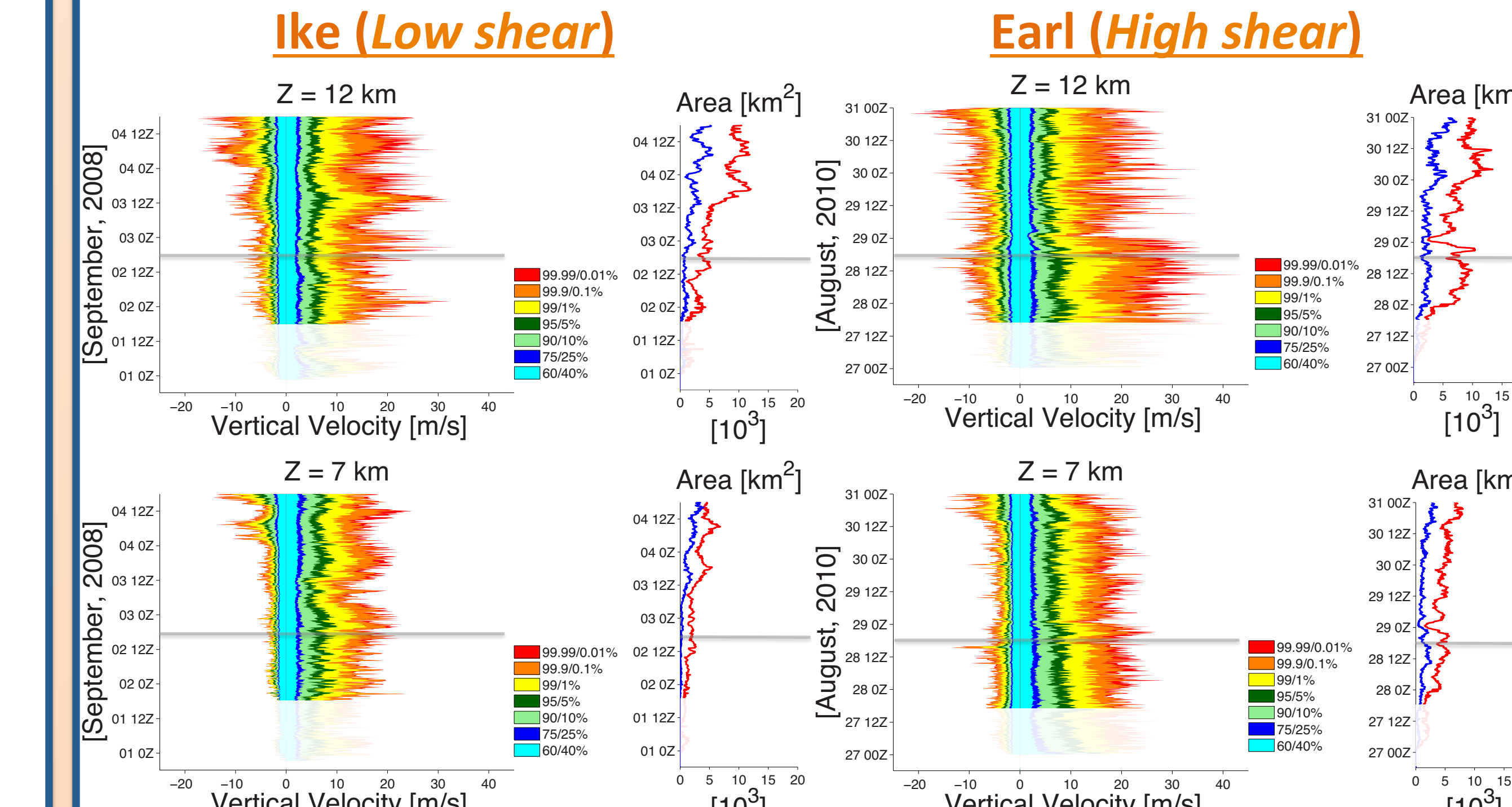


Fig. 4: Cumulative contoured frequency by time diagrams of vertical velocity (left) and areal coverage (right) of updrafts ($W \geq 1 \text{ m s}^{-1}$) and downdrafts ($W \leq -1 \text{ m s}^{-1}$) at 12 km (top) and 7 km (bottom). Each over innermost 1°.

Results: Heating Structures

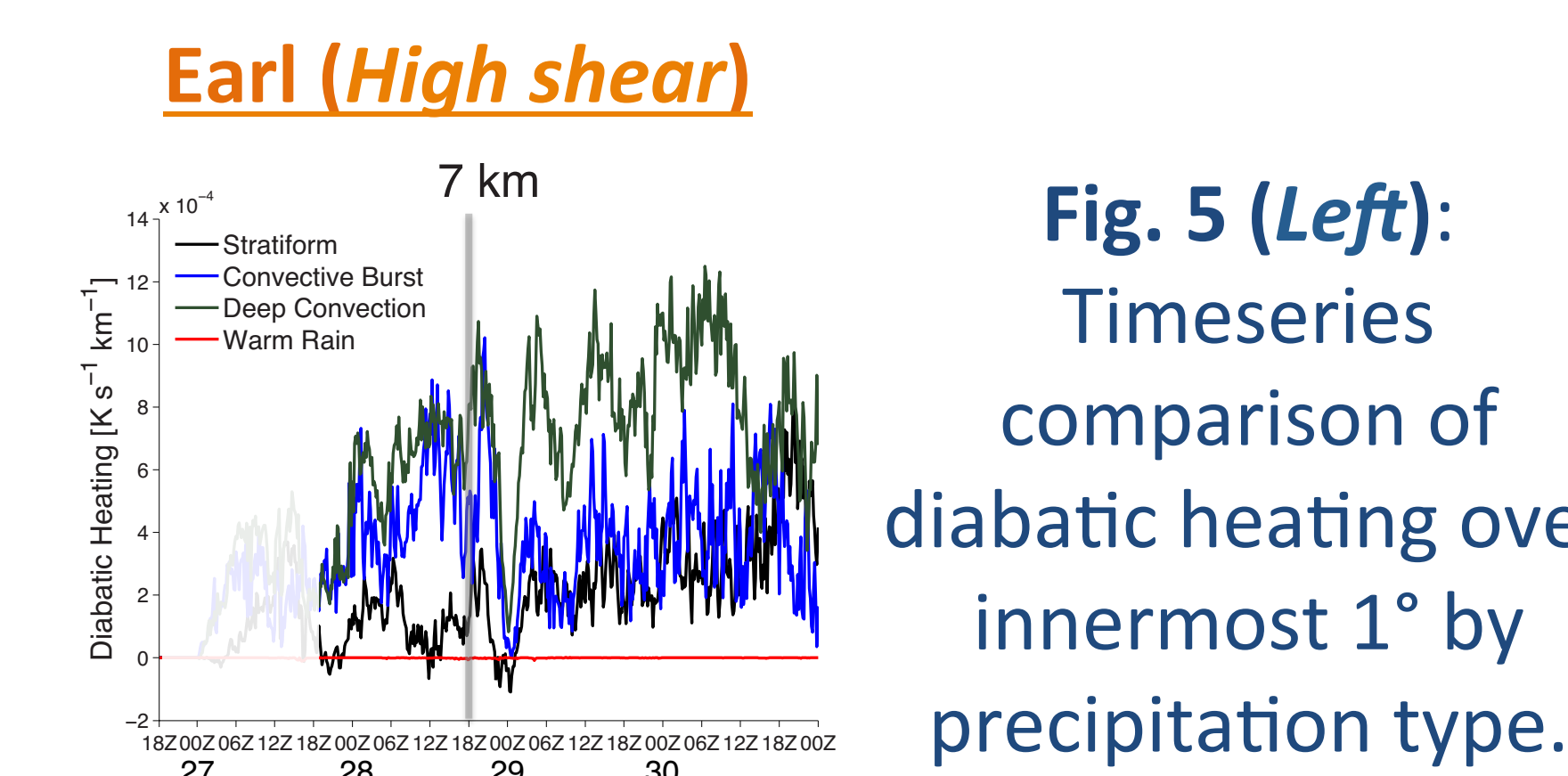


Fig. 5 (Left): Timeseries comparison of diabatic heating over innermost 1° by precipitation type.

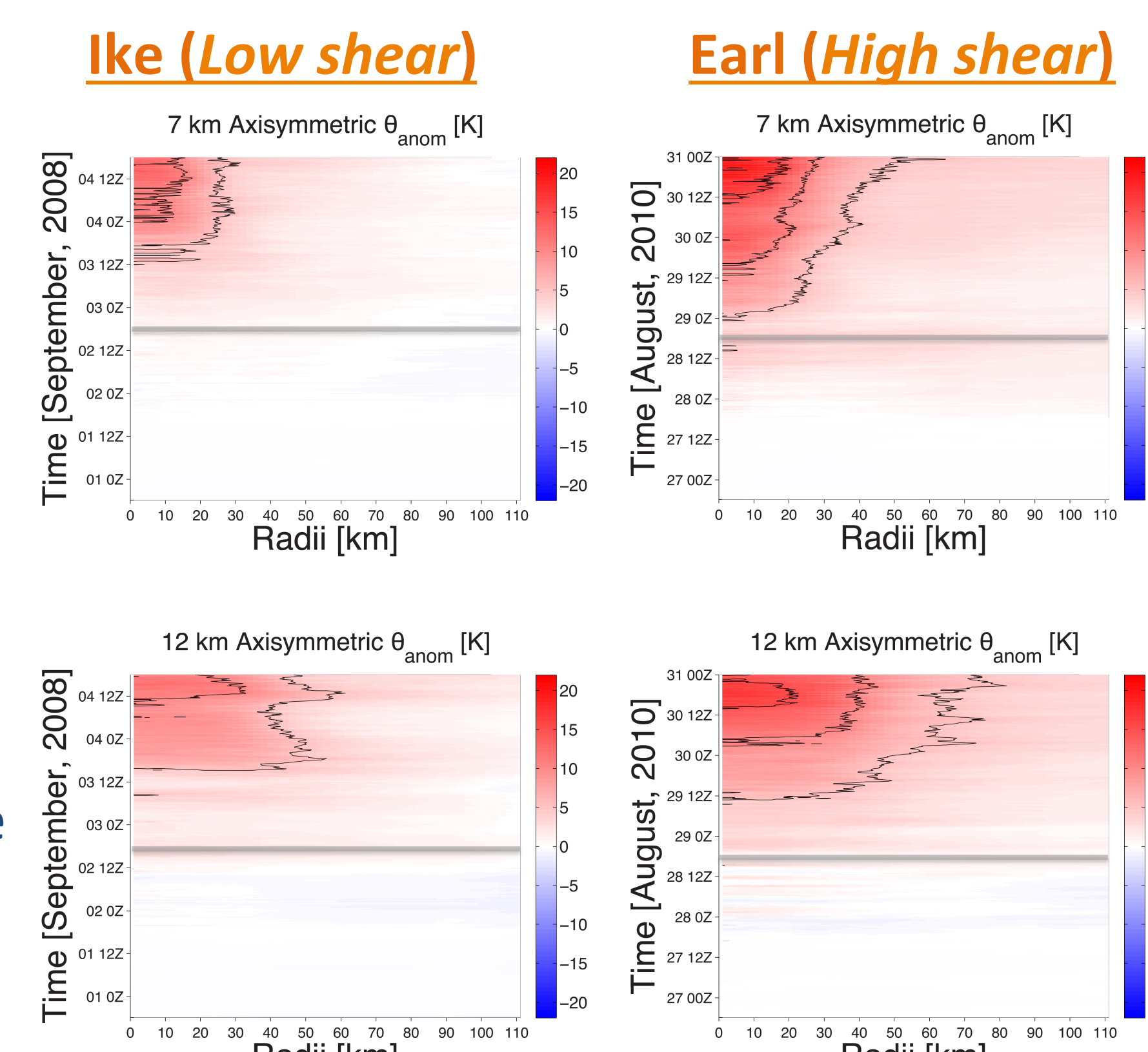
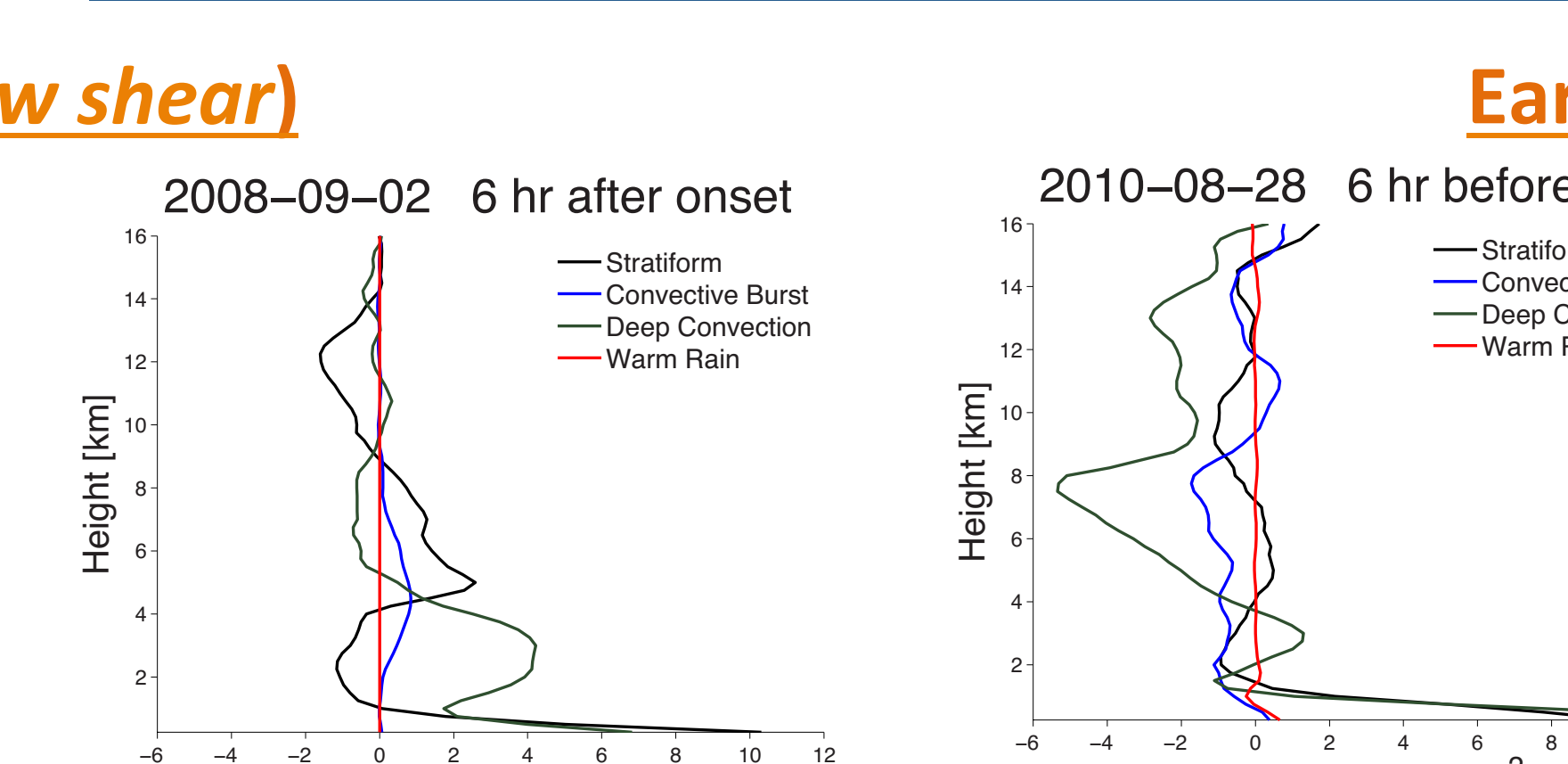


Fig. 6 (Right): Axisymmetric potential temperature anomaly evolution (relative to end of spin-up). Black lines at 5K intervals.

Results: Precipitation Type Spin-Up Contribution



Model Simulation Conclusions

Bursts: Prior to RI, Ike lacks a signature, whereas Earl sees increased activity (Fig. 2, 3). Ike catches up 18-28 h after RI onset.

Diabatic heating: Ike is primarily driven by stratiform and non-burst convection (Fig. 5); Earl's bursts contribute to half of the heating.

Spin Up: Ike spins up at low- and mid-levels (Fig. 7), by divergence (Fig. 8). Earl spins at low-levels (Fig. 7) by divergence and shearing (Fig. 8).

Warm Rain: There is a negligible contribution to both heating (Fig. 5) and spin-up (Fig. 9) from warm rain, with no spatial trend exhibited (Fig. 3).